Electronic Supplementary Information for

Prussian blue derived Fe_2N for efficiently improving photocatalytic hydrogen evolution activity of g-C_3N_4 nanosheets

Weiliang Qi, [a] Siqi Liu,*[b,c] Fei Li,*[a] Heng Jiang,*[a] Zhixing Cheng, [b,c] Shanlin Zhao [a] and Minghui Yang*[b,c]

[a]*College of Chemistry, Chemical Engineering and Environment Engineering, Liaoning Shihua University, Fushun 113001, PR China*

[b]*Ningbo Institute of Materials Technology and Engineering, Chinese Academy of Sciences, Ningbo 315201, PR China*

[c]*Center of Materials Science and Optoelectronics Engineering, University of Chinese Academy of Sciences, Beijing 100049, China*

*[a]*E-mail: weizn@126.com, hjiang78@hotmail.com.*

*[b,c]*E-mail: myang@nimte.ac.cn, liusiqi@nimte.ac.cn.*

Table of contents

I.Experimental Procedures

Electrochemical Measurements: The electrochemical tests were conducted on an electrochemical workstation (CHI760E, CH Instrument) with a conventional three electrode cell. A Pt plate was employed as the counter electrode and an Ag/AgCl electrode was used as the reference electrode. The working electrode was prepared on fluorine-doped tin oxide (FTO) glass that was cleaned by sonication in ethanol for 30 min and dried at 353 K. The boundary of FTO glass was protected using the scotch tape. The 5 mg sample and 30 μL Nafion solution (5 wt%) were dispersed in 1 mL of DMF by sonication to get slurry. Then, 40 μL of slurry was spread onto the pretreated FTO glass. After air at room temperature, the working electrode was further dried at 393 K for 2 h to improve adhesion. Then, the scotch tape was unstuck, and the uncoated part of the electrode was isolated with epoxy resin. The exposed area of the working electrode was 0.25 cm^2. The photocurrent measurements were carried out with the electrolyte was 0.2 M aqueous Na_2SO_4 solution. The electrochemical impedance spectroscopy (EIS) measurements were performed in 0.2 M aqueous Na_2SO_4 solution by applying an AC voltage with -1.3 mV amplitude in a frequency range from 1 Hz to 100 kHz. The polarization curve is performed in the same above mentioned three-electrode system, while the bias sweep range is from -1.6 to 0 V vs Ag/AgCl the electrolyte was 0.2 M aqueous Na_2SO_4 solution.

II.Supplementary illustrations and explanations

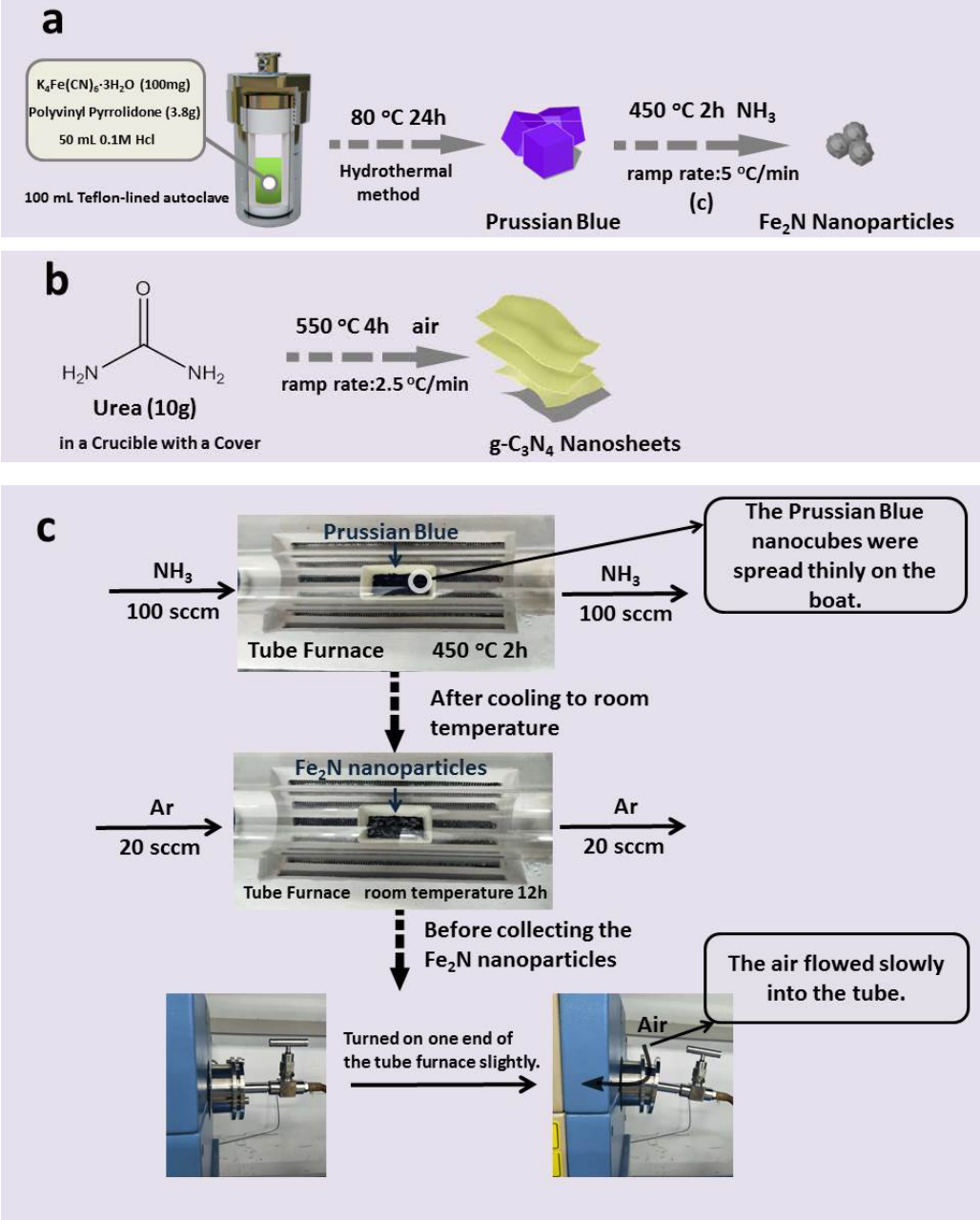

Scheme S1. The schematic illustration for the preparation of Fe_2N and g-C_3N_4 nanosheets.

Note: Scheme S1 c is the concrete step and matters need attention of the synthesis of Fe_2N nanoparticles by Prussian Blue nanocubes.

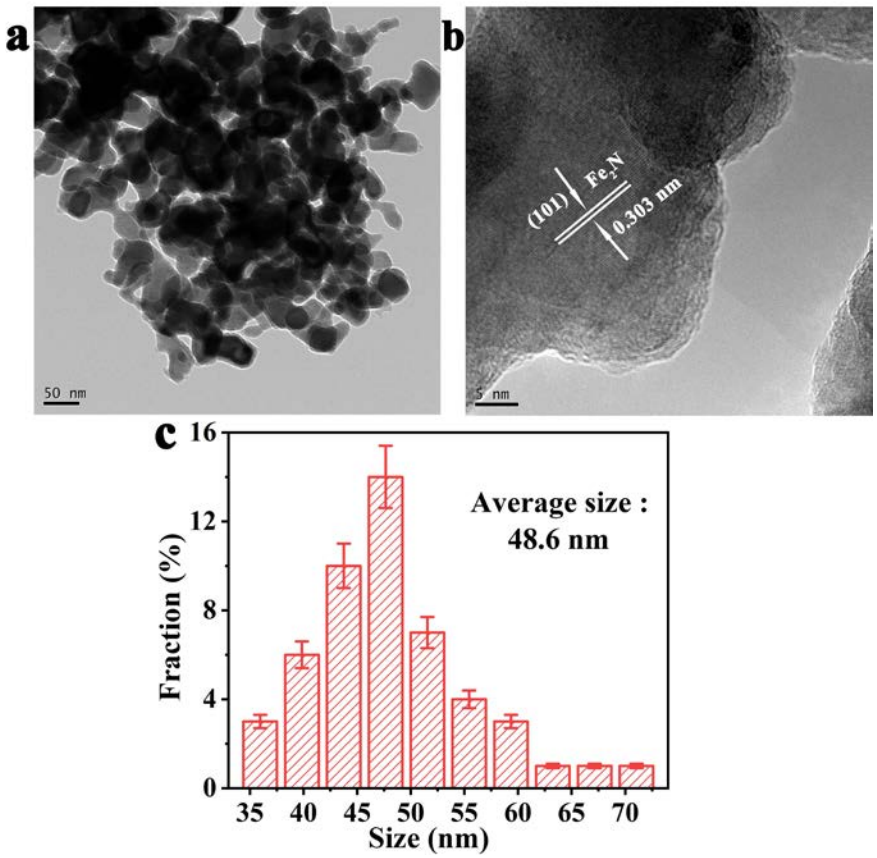

Fig. S1 (a) TEM and (b) HRTEM images image of Fe_2N nanoparticles. (c) The diameters statistic histogram of Fe_2N Nanoparticles.

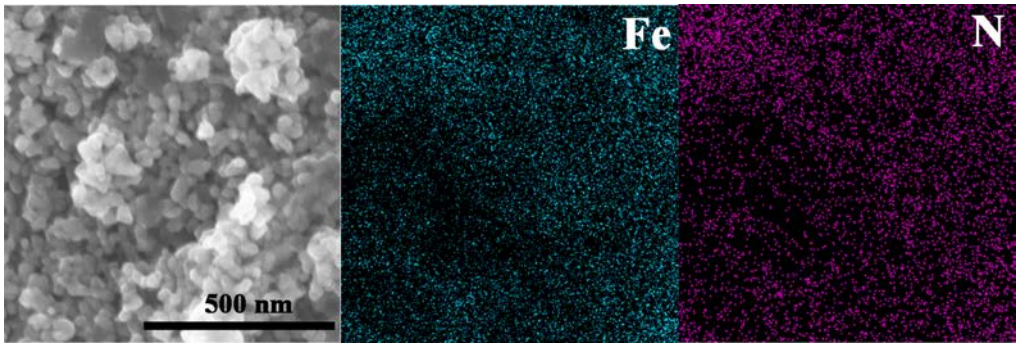

Fig. S2 The EDS mapping of the Fe_2N nanoparticles.

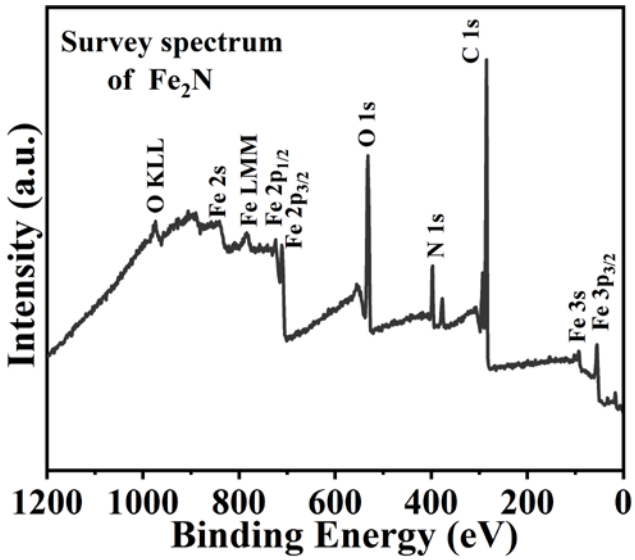

Fig. S3 The X-ray photoelectron survey spectrum of Fe_2N nanoparticles.

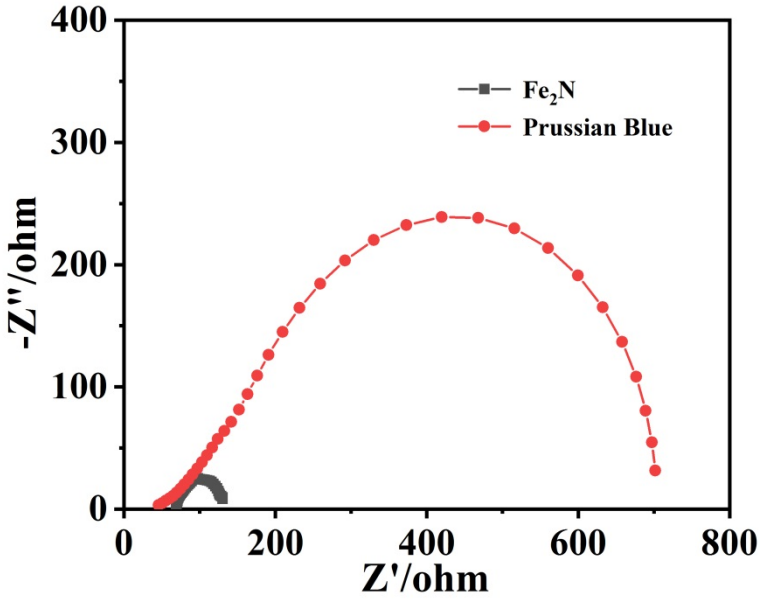

Fig. S4 Electrical impedance spectra of Prussian Blue nanocubes and Fe_2N nanoparticles.

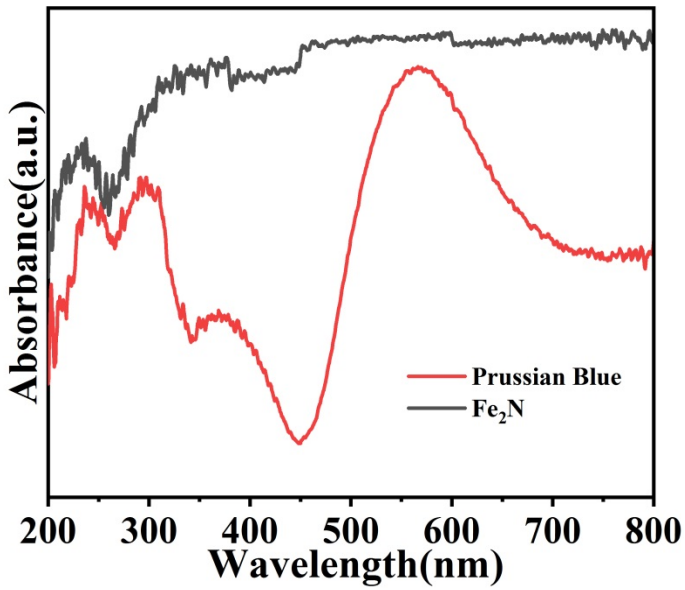

Fig. S5 UV-vis absorption spectra of Prussian Blue nanocubes and Fe_2N nanoparticles.

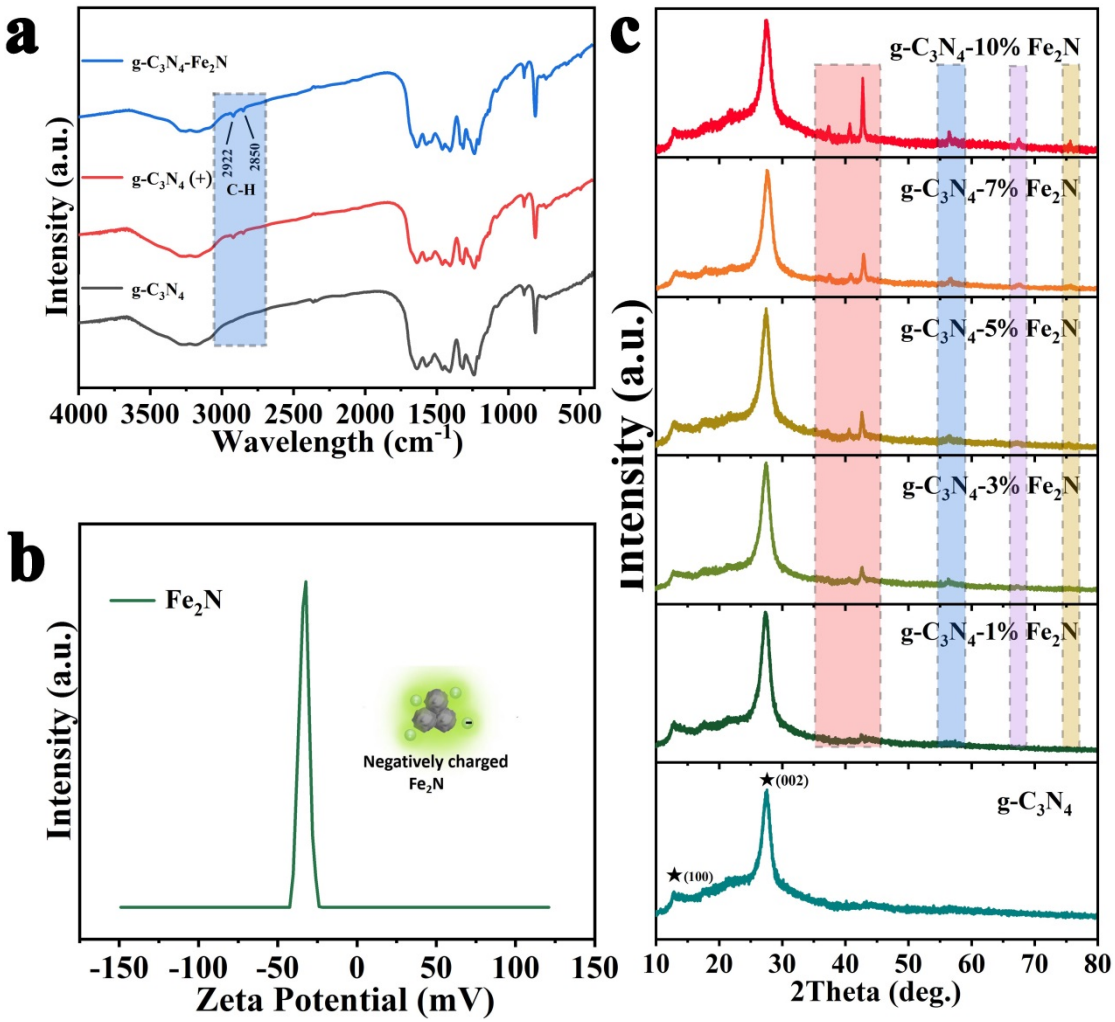

Fig. S6 (a) The FT-IR spectra of pure g-C_3N_4, CTAB modified g-C_3N_4 and g-C_3N_4-Fe_2N nanocomposites. (b) Zeta potential measurements of Fe_2N nanoparticles. (c) XRD pattern of pure g-C_3N_4 and a series of g-C_3N_4-Fe_2N nanocomposites.

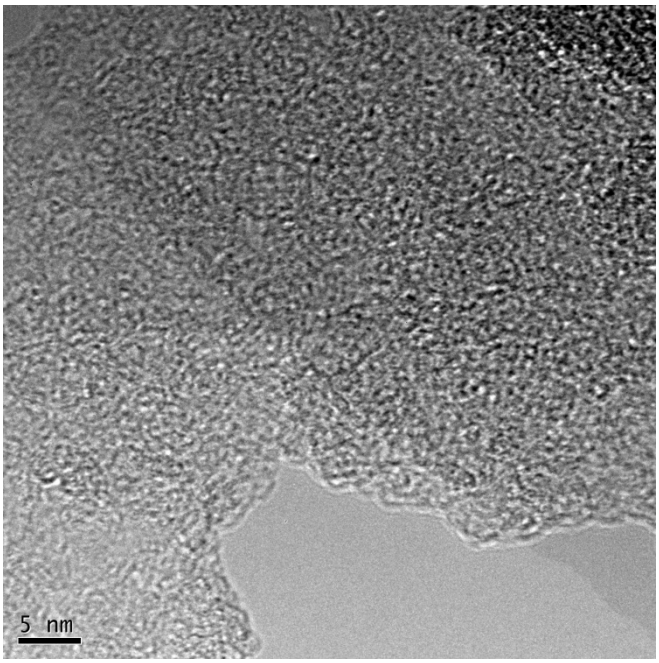

Fig. S7 HRTEM image of pure g-C_3N_4 nanosheets.

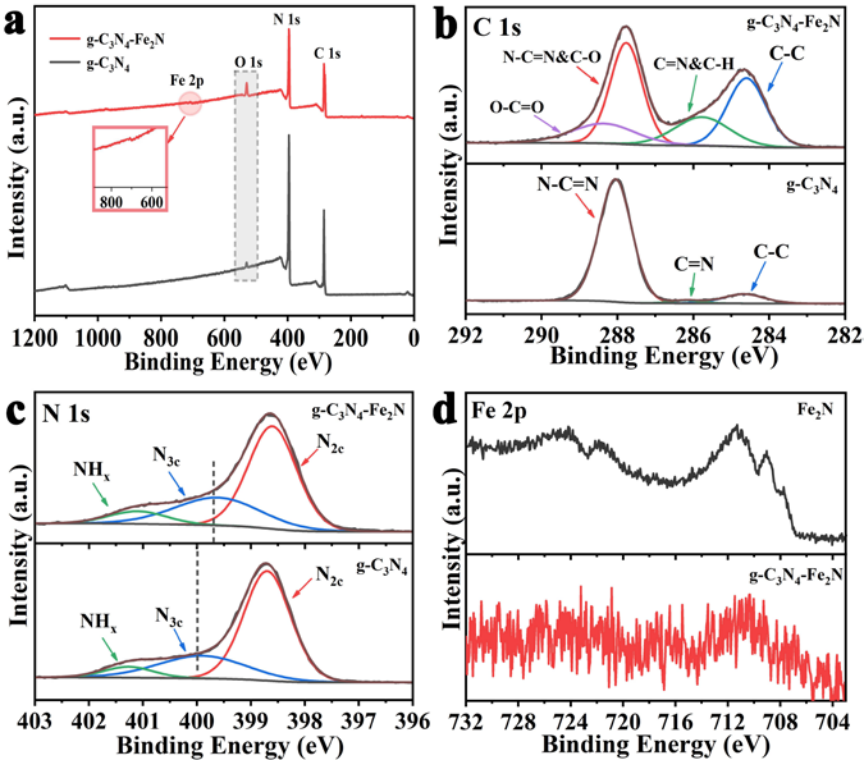

Fig. S8 (a) The X-ray photoelectron survey spectrum of g-C_3N_4 and g-C_3N_4-Fe_2N. High-resolution spectrum of (b) C 1s and (c) N 1s for g-C_3N_4 and g-C_3N_4-Fe_2N. High-resolution spectrum of (d) Fe 2P for g-C_3N_4-Fe_2N and pure Fe_2N.

Note: The peak of O 1s of the g-C_3N_4-Fe_2N nanocomposite is an obvious stronger than that of the pure g-C_3N_4, in the survey spectrum. It has been proved to be the result of the modification on the surface of the g-C_3N_4 by the CTAB. Meanwhile, the g-C_3N_4-Fe_2N nanocomposite has an extra peak at 708 eV corresponding to the Fe 2p.

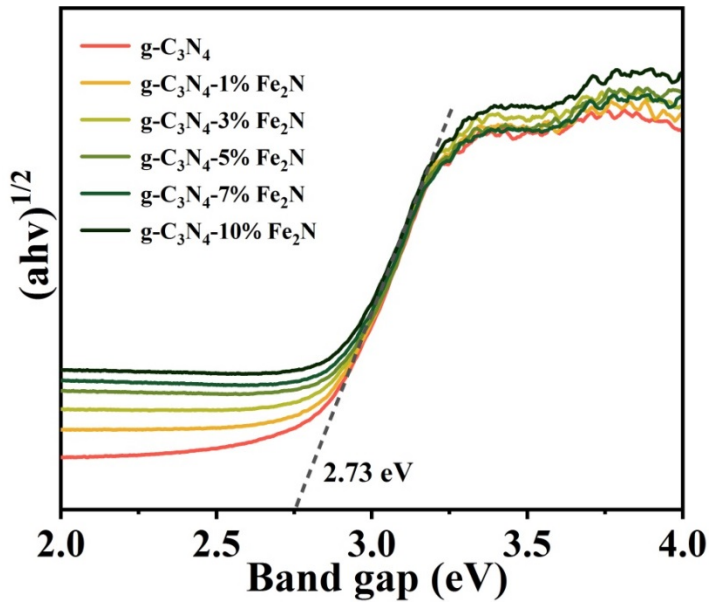

Fig. S9 Tauc plots of the UV–vis spectra for a series of samples.

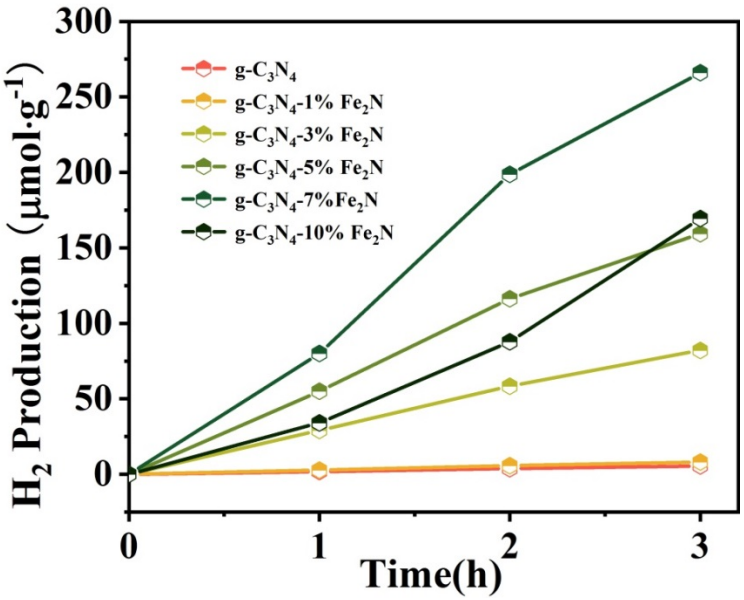

Fig. S10 Time-dependent photocatalytic H_2 evolution over the g-C_3N_4-Fe_2N nanocomposites with different ratio of Fe_2N.

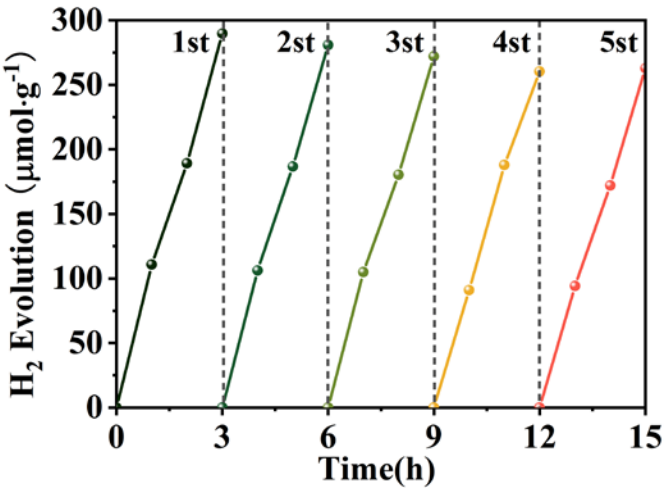

Fig. S11 Stability examination of H_2 production (evacuation every 3 h) for the g-C_3N_4-7%Fe_2N sample.

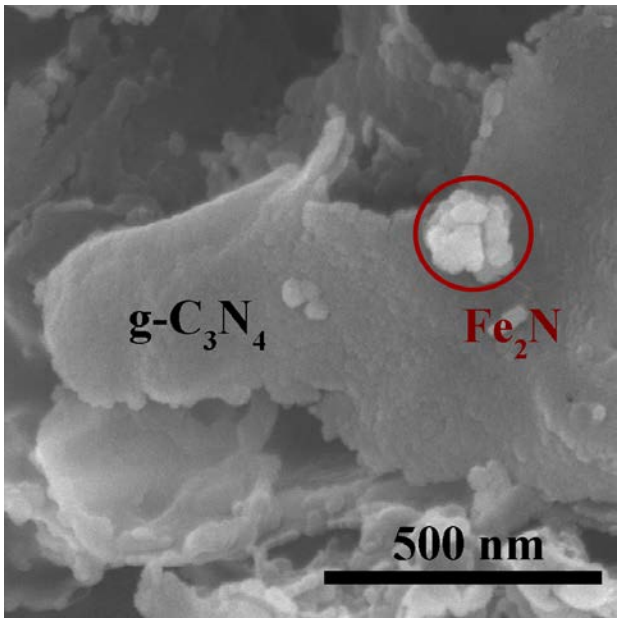

Fig. S12. The SEM image of the reacted g-C_3N_4-7%Fe_2N sample.

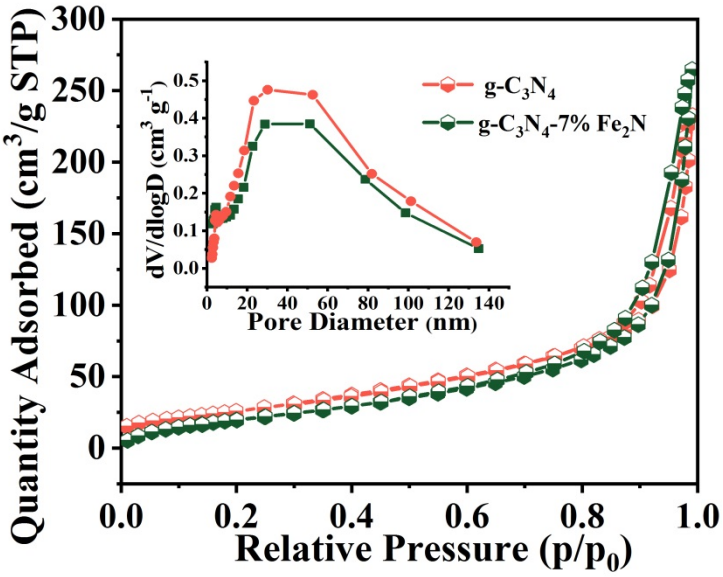

Fig. S13. N_2 adsorption–desorption isotherms and the corresponding pore size distribution curves (inset) of g-C_3N_4 and g-C_3N_4–7%Fe_2N.

Table S1. Pore Structure Parameters of g-C_3N_4 and g-C_3N_4-7%Fe_2N.

Photocatalyst	BET surface area ($m^2\ g^{-1}$)	mean pore diameter (nm)	pore volume ($cm^3\ g^{-1}$)
g-C_3N_4	97.96	14.66	0.38
g-C_3N_4-7%Fe_2N	81.11	16.49	0.44

Table S2. Representative summary on photocatalytic activity of non-noble based photocatalysts toward water splitting H_2 evolution.

Photocatalyst	Co-catalysts/ mass ratio	Light source	Reaction conditions	PHER rate[a]	Ref.
g-C_3N_4	Ni_xP_y /5 wt%	Xe light 300W, λ>420 nm	Aqueous TEOA solution (25%)	34	[S1]
CdS	NiC /1 wt%	Xe light 350W, λ>420 nm	Aqueous solution of Na_2S (0.25 M) and Na_2SO_3 (0.25 M)	7.76	[S2]
CdS/g-C_3N_4	$Ni(OH)_2$ / 4.76 wt%	Xe light 300W, λ>420 nm	Aqueous solution of Na_2S (0.5 M) and Na_2SO_3 (0.7 M)	25.65	[S3]
$ZnIn_2S_4$	MoC-QDs/C / 2.5 wt%	Xe light 300W, λ>400 nm	Aqueous lactic acid solution (10%)	48	[S4]
g-C_3N_4	CoO	Xe light 300W, λ>400 nm	Aqueous lactic acid solution (10%)	3	[S5]
CdS	Mo_2C@C / 2 wt%	Xe light 300W, λ>420 nm	Aqueous lactic acid solution (10%)	26	[S6]
g-C_3N_4	$Ni_xCo_{1-x}S_2$ / 5 wt%	White LED, λ>420 nm	Aqueous TEOA solution (15%), Eosin Y-sensitized catalyst (10mg)	9.08	[S7]
CdS	MoS_2 / 2 wt%	Xe light 300W, λ>420 nm	Aqueous lactic acid solution (10%)	64.9	[S8]
g-C_3N_4	Fe_2N / 7 wt%	Xe light 300W, λ>400 nm	Aqueous TEOA solution (10%)	**48**	**This work**

Note: [a]**PHER rate** denotes the hydrogen evolution rate of times higher than pristine photocatalyst.

III.Supplementary References:

[S1] Z. Sun, M. Zhu, M. Fujitsuka, A. Wang, C. Shi, T. Majima, ACS Appl Mater Interfaces, 9 (2017) 30583-30590.

[S2] S. Ma, Y. Deng, J. Xie, K. He, W. Liu, X. Chen, X. Li, Applied Catalysis B: Environmental, 227 (2018) 218-228.

[S3] Z. Yan, Z. Sun, X. Liu, H. Jia, P. Du, Nanoscale, 8 (2016) 4748-4756.

[S4] F. Gao, Y. Zhao, L. Zhang, B. Wang, Y. Wang, X. Huang, K. Wang, W. Feng, P. Liu, Journal of Materials Chemistry A, 6 (2018) 18979-18986.

[S5] Z. Mao, J. Chen, Y. Yang, D. Wang, L. Bie, B.D. Fahlman, ACS Appl Mater Interfaces, 9 (2017) 12427-12435.

[S6] Y.-X. Pan, J.-B. Peng, S. Xin, Y. You, Y.-L. Men, F. Zhang, M.-Y. Duan, Y. Cui, Z.-Q. Sun, J. Song, ACS Sustainable Chemistry & Engineering, 5 (2017) 5449-5456.

[S7] K. Fan, Z. Jin, H. Yang, D. Liu, H. Hu, Y. Bi, Sci Rep, 7 (2017) 7710.

[S8] B. Han, S. Liu, Y.-J. Xu, Z.-R. Tang, Applied Catalysis B: Environmental, 202 (2017) 298-304.